# INVESTIGATION OF THE DETECTIVITY OF RADIATION-PRODUCED DEFECT LEVELS IN n- AND p-TYPE SILICON AND GERMANIUM

Semiannual Progress Report

Grant No. NGR-47-005-093

National Aeronautics and Space Administration

Submitted by:

Robert J. Mattauch



Research Laboratories for the Engineering Sciences

University of Virginia

Charlottesville

Report No. EE-4031-102-69U

March 1969

# INVESTIGATION OF THE DETECTIVITY OF RADIATION-PRODUCED DEFECT LEVELS IN n- AND p-TYPE SILICON AND GERMANIUM

Semiannual Progress Report

Grant No. NGR-47-005-093

National Aeronautics and Space Administration

Submitted by:

Robert J. Mattauch

Division of Electrical Engineering

RESEARCH LABORATORIES FOR THE ENGINEERING SCIENCES

SCHOOL OF ENGINEERING AND APPLIED SCIENCE

UNIVERSITY OF VIRGINIA

CHARLOTTESVILLE, VIRGINIA

Report No. EE-4031-102-69U

March 1969

Copy No. 5

TABLE OF CONTENTS

LIST OF FIGURES

# SECTION I
# INTRODUCTION AND SUMMARY

This report reflects the progress made since the submission of the first Semiannual Progress Report in August 1968.

The progress in the six-month period being reported has involved four main divisions:

1) the final development of a system for the determination of black-body responsivity, including the development of a low-noise, transistorized preamplifier capable of measuring signal voltages in the 100 microvolt region across a device of resistance in the $10^9\Omega$ region.

2) the collection, processing, and interpreting of black body data.

3) re-evaluation of the spectral system originally planned leading to the design and development of a system which incorporates both spectral and black body capabilities.

4) the collection, processing, and interpretation of data to relate the capabilities of the detector and the primary cause of photoconduction in the detector.

The report is divided into five sections not including the present one: One section is devoted to theory and the remaining four are devoted to the above mentioned topics.

Black-body data has been collected on devices of n-type silicon with resistivities of 1 ohm-cm 0.1 ohm-cm and .03 ohm cm and of p-type silicon with resistivities of 0.1, 1, and 10 ohm-cm. The bulk of the data has been taken on N 1.0 samples since this type and resistivity seems to provide, on the average, better black-body responsivities. The current voltage characteristics of the p-type devices have been found to be slightly non-linear with the Ni contacts presently used at liquid nitrogen temperatures, this being especially true of the 1 Ωcm p-type devices. One ohm-cm n-type devices whose liquid nitrogen temperature resistances varied from $5.0 \times 10^7\Omega$ to $3.5 \times 10^{10}\Omega$

were examined. The effects of annealing such devices were examined, and the results will be presented. From this data, definite trends were established concerning the effect of frequency of incident radiation, of bias voltage across the device, and of annealing on the black body responsivity.

The development of the spectral system has enabled the researcher to have at his disposal, a source of monochromatic electromagnetic radiation variable from 1μ to 20μ by the utilization of four different diffraction gratings. From this system, the peak spectral response of devices in the region of 1-4μ has been established. This information and that obtained by the use of windows of various spectral transmission (as verified by infrared spectrophotometer measurements) has allowed the establishment of the wavelength range of operation of the detector. A computer program has been perfected which will yield a plot of $D^*(\lambda)$ (spectral detectivity) as a function of wavelength from the data obtained from this system. The system has been designed incorporating a smaller black body source and dewar mount so that either black body or spectral data may be obtained by simply rotating the dewar so that the appropriate source is used.

With the perfection of the computer program, further work is being carried out involving the spectral detectivity as a function of type, resistivity, and annealing of devices. An investigation of the kinetics of the physical processes involved in the observed photoconductivity will be carried out.

## SECTION II
## THEORY

This material is presented as a review of the section on theory presented in the 1st semiannual report and parallels the former presentations greatly. It basically presents the theory of determining the presence and degree of photoconductivity in the detector.

In evaluating a device as a photoconductor, one usually assesses its relative value on the basis of figures of merit. The most important of these figures are responsivity and detectivity. Responsivity is the measure of the ratio of the output rms signal voltage to the rms radiant power, W, incident on the detector; while detectivity, generally speaking, gives a measure of rms signal-to-noise ratio per unit of incident radiant power. Thus the noise of the detector is the limiting factor of detectivity. The following is a brief account of the techniques being used to determine the device noise, N(f), spectral responsivity, $R(\lambda)$, and spectral detectivity $D^*_\lambda$.

### A. Noise

As pointed out in the 1st semiannual report, the device sensitivity is limited by (a) current noise, (b) circuit noise, (c) generation-recombination noise, and (d) background noise.

In the experimental configuration, noise is obtained as a function of frequency and bias over the desired ranges. No problems have arisen with circuit, or background noise, due to the fact that the background noise is generally of a magnitude less than a microvolt whereas device noise generally is of the order of $10^1$ to $10^2$ microvolts.

### B. Responsivity

The responsivity, R, of a photoconductor is defined as the ratio of the open circuit rms signal voltage, $V_s$, to the rms radiant power, W, incident on the detector. It is a function of the temperature and bias of the device as well as the chopping frequency and spectral content of the source.

To determine the spectral responsivity $R(\lambda)$ the device black body responsivity, the device output voltage, $E_1$, and the output of a constant responsivity thermal detector $E_2$ as a function of wavelength, $\lambda$, must be determined. $R(\lambda)$ is then given by

$$R(\lambda) = Rbb \frac{L(\lambda)P_{rms}}{\int L(\lambda)P(\lambda)_{rms} d\lambda}$$

where $P(\lambda)_{rms}$ is the spectral power of $P_{rms}$, the black body power

and $$L(\lambda) = \frac{E_1(\lambda)}{E_2(\lambda)}$$

where $E_1$ = Device output due to a spectral source

$E_2$ = Bolometer output due to a spectral source*

C. Detectivity

The spectral detectivity $D^*_\lambda$ is now found by means of the relation

$$D^*_\lambda = (Af)^{1/2} R(\lambda)/N_{rms}$$

where A = the adopted device area

f = the noise bandwidth

and $N_{rms}$ = the noise voltage at the maximum bais, maximum chopping frequency values.

*The responsivity of the bolometer element is assumed constant as stated by the manufacturer.

## SECTION III

## SYSTEM AND TEST PROCEDURES FOR BLACK-BODY RESPONSIVITY

The basic system has been changed slightly from the one mentioned in the 1st semiannual report. The most notable exception is the replacement of the Tektronix Type 122 preamplifier of input impedance of 10 mΩ, by a transistorized amplifier of input impedance greater than 500 mΩ and which has a negative effective input capacitance due to a capacitance feedback loop which enables the capacitance of the dewar and device leads to be "tuned out." This negative capacitance circumvents any problem with undesirable RC time constants due to the high resistance of the device and low capacitance of the device leads.

The system contains a black body source, as discussed in detail in the 1st semiannual report, which is maintained at a constant 500°K. The black body was constructed from a cylindrical block of copper as outlined in Kruse et al. [1] This block is heated by a cylindrical bore furnace, the temperature of which is controlled. A water cooled collimator is placed at the end of the furnace bore a known distance from the black body. Between this collimator and the device is mounted a chopper capable of modulating the source intensity at frequencies as high as 1350 Hz. The device to be tested is mounted in a dewar in front of the black body collimator. A germanium window, which transmits ~50% of the incident radiation as verified by spectrophotometeric tests, is in the optical path between the collimator and detector. The detector-source distance is maintained at 0.1 m. The radiant energy incident on the device, and the amplitude of any harmonic of the chopping frequency can be found as previously reported. A HP H21-521A counter is used to monitor the chopper frequency.

The detector is in series with a bias source, load resistor, and calibration resistor. The load resistor is fixed at 50 mΩ and the calibration resistor at 50 Ω. The bias supply used is a John Fluke model 407 power supply with an additional RC filter for decreasing 60 Hz. harmonics amplitudes. The calibration voltage is fed into the calibration resistor from a Hewlett-Packard model 651A test oscillator. The output is fed into the transistorized amplifier through a blocking capacitor (see Fig. 1). The amplifier provides an input impedance on

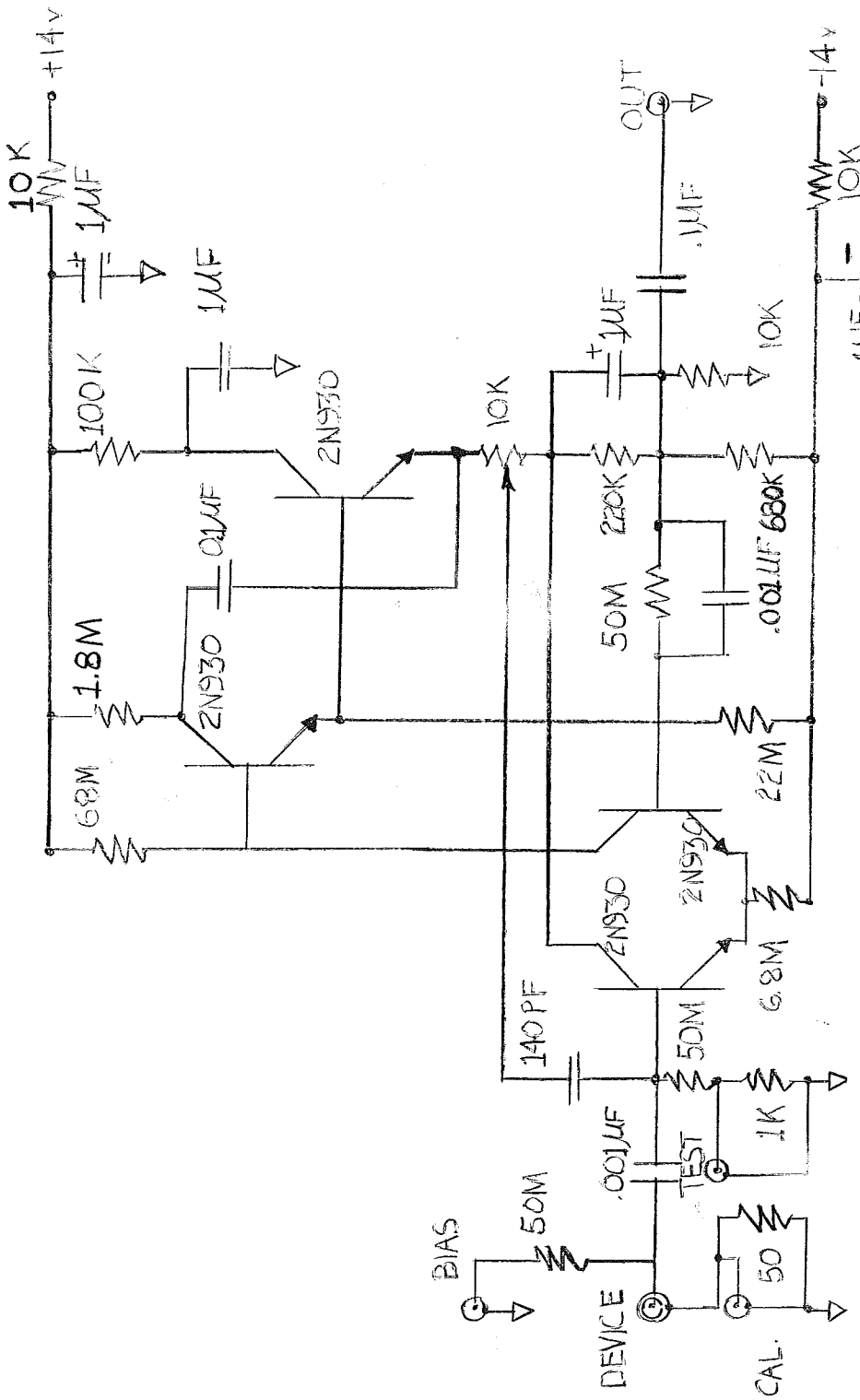


Figure 1 Schematic Diagram of Biasing Circuit and Preamplifier

the order of 500 mΩ and an output impedance of 10K. The capacitance feedback loop provides a "negative" capacitance to "tune-out" capacitance in the device leads. Both the biasing circuit and amplifier depicted in Fig. 1 are enclosed in an [CU-2100-A] aluminum box which is mounted directly onto the dewar. Neither side of the device is grounded, so the dewar is held by an insulated mount in front of the black-body. The output is monitored by a Tektronix Type 317 oscilloscope and is also fed into a BNC switch. Connected to the other side of the switch is the signal generator output. The switch output is then fed into the HP302A wave analyzer. A block diagram of the completed system appears in Fig. 2.

The test procedure for obtaining Rbb is as follows:

(1) The device output without regard to amplifier gain is taken as a function of frequency and bias voltage.

(2) The corrected device output is found by removing the device from the infrared path, feeding a calibration signal into Rcal from a signal generator at the same infrared chopping frequency and with the same bias across the device. Once the calibration signal has been adjusted so that the output signal is equal in value (amplitude and frequency) to that previously noted, the signal output from the signal generator which is the open circuit device output is determined. This measurement is facilitated by the BNC switching arrangement previously mentioned.

(3) The noise of the device is then obtained by the procedure previously outlined in the 1st semiannual report. The noise root power spectrum may then be found by the relation given by Eisenman [2]:

$$N(f) = \left[\frac{E_T^2(f) - E_c(f)^2}{g^2}\right]^{1/2} \Delta f$$

where $E_T$ = the noise voltage obtained from the output with the device in the circuit, as a function of frequency.

$E_c(f)$ = obtained with the device shorted (circuit noise)

$g$ = the circuit gain obtained from $V_{out}/V_{cal}$

$\Delta f$ = the noise bandwidth of wave analyser used.

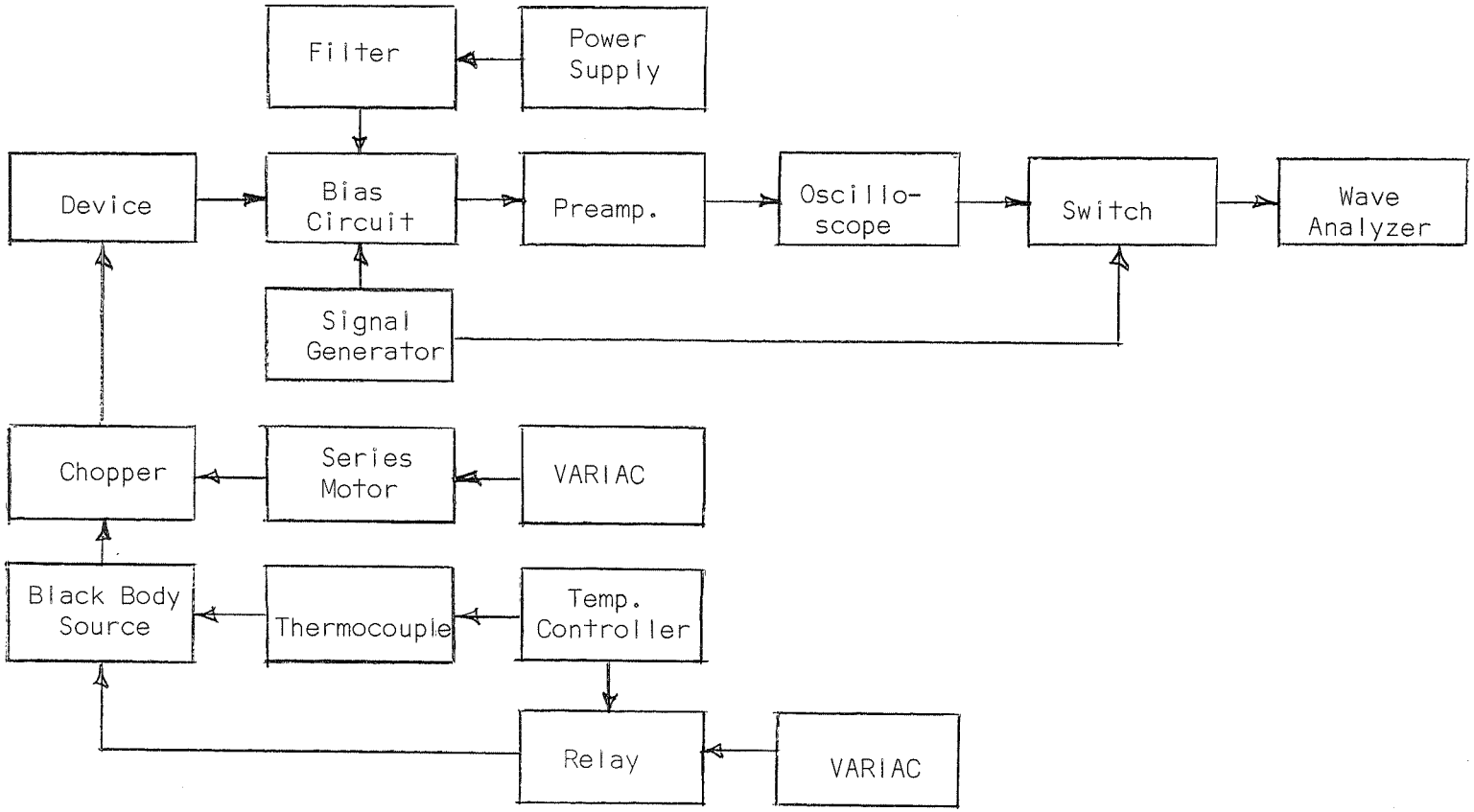


Figure 2 Block Diagram of Responsivity and Frequency Response Equipment

Rbb is obtained from the previous measurements by means of the relation

$$Rbb = \frac{V(rms)}{J(rms)A}$$ where now $V_{rms} = V_{cal}$ or the corrected device output

J = rms value of the fundamental component of the incident energy flux

A = adopted area of the detector

$V(rms) = V_{cal}$ is the rms value of the fundamental component of the output voltage referred to the open-circuit device terminals.

As outlined previously, the rate of flow of energy onto the device surface has been found to be $2.24 \times 10^{-5}$ watts. The amplitude of any harmonic can be found from the work of McQuistan [3]. The expression for the first harmonic is

$$A = I_0 \frac{4Rr}{\pi} J_1(\frac{R}{2r}) \sin \frac{\pi}{2}$$

where

R = radius of collimator

r = half the chopping tooth width where the tooth-notch ratio is unity

$J_1$ = 1st order Bessel fn.

$I_0$ = radiation incident on the chopper

A = $0.203\ I_0$ so that the fundamental of the radiation incident on the device can be written as

$$W_1 = 0.454 \times 10^{-5} \cos \omega t.$$

## SECTION IV
## BLACK BODY DATA AND INTERPRETATION

Verification of the fact that silicon devices which had been exposed to high energy electron radiation exhibited photoconductivity due to the radiation-induced levels was first made by means of black-body responsivity tests.

The system used to obtain data for black body responsivity having been discussed, the resulting data will now be presented. A device output was found from all six of the resistivities and types of silicon tested. These were 10, 1, and 0.1 ohm-cm p-type and 1.0, 0.1, and 0.3 ohm-cm n-type.

The test procedures outlined above were used and the black body radiation was modulated over the range 30-1100 Hz. while the device bias used was 100, 300, and 500 volts. Shown in Figs. 3 through 8 are sample curves of responsivity versus black-body radiation modulation frequency for each of the three resistivities of each type of silicon used. Fig. 3 shows a curve of Rbb vs. f for a sample 1.0 ohm-cm n-type device and is typical of all curves of the devices tested in that the responsivity increased with decreasing radiation modulation frequency. In each case the black-body responsivity was calculated by the method outlined in Section III of this report. For example, device number 329N1.0 was tested at 100 Hz. with 500 volt bias. The calibrated output was $9.52 \times 10^{-2}$ volts and the rms value of power incident on the device was $2.24 \times 10^{-5}$ watts yielding a black-body responsivity of $47 \times 10^{2}$ volts $watt^{-1}$. The resistance of that particular device at 77°K was found to be $7.7 \times 10^{8}$ ohms. Figs. 4, 5, 6, 7, and 8 present curves of Rbb vs. f for a 0.1 ohm-cm n-type device whose 77°K resistance was $3.3 \times 10^{8}$ ohms, 10 ohm-cm p-type device whose 77°K resistance was $8 \times 10^{11}$ ohms, 1.0 ohm-cm p-type device whose 77°K resistance was nonlinear, 0.1 ohm-cm p-type device whose 77°K resistance was $7.0 \times 10^{4}$ ohms, and a .03 ohm-cm n-type device whose 77°K resistance was $2.2 \times 10^{11}$ ohms.

Because of a nonlinearity in current-voltage characteristics at 77°K of devices fabricated from at least one resistivity p-type material the devices fabricated from 1.0 ohm-cm n-type material were used almost exclusively in annealing studies. Annealing was first employed as a means of decreasing the

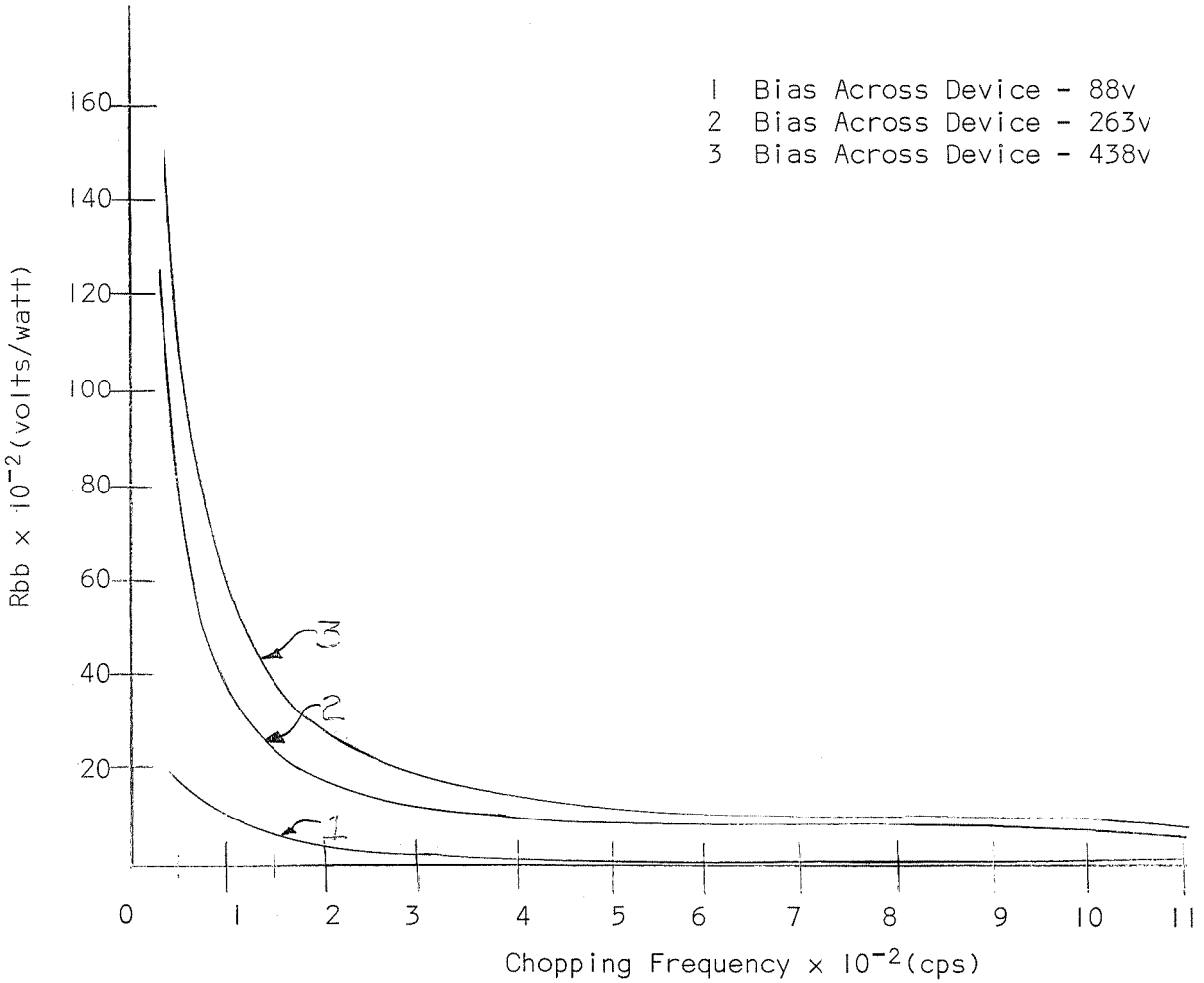


Figure 3 Black Body Responsivity vs. Chopping Frequency for a Typical n-Type Device Whose Initial Resistivity was 1 Ωcm. (Device 329N1.0)

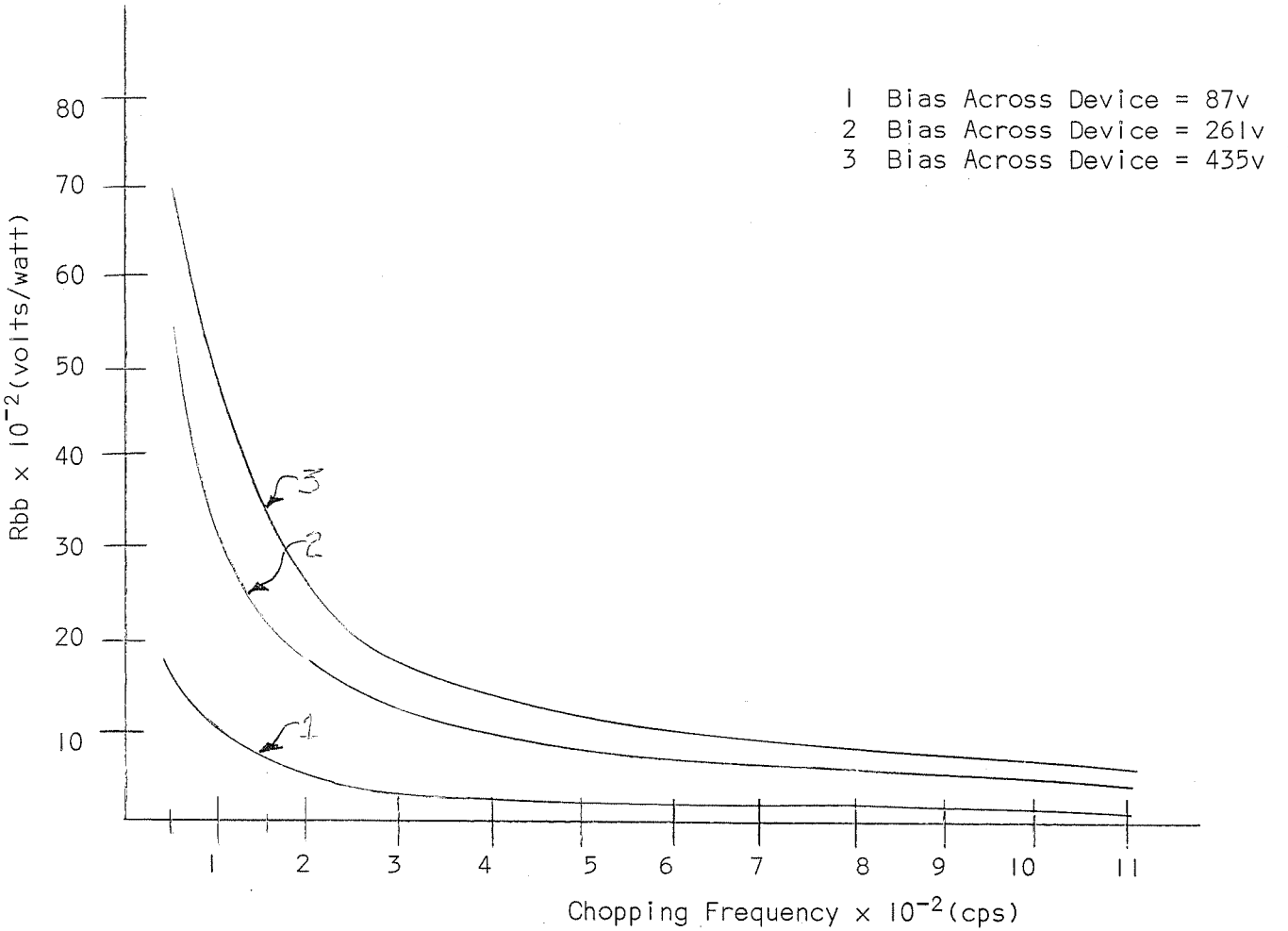


Figure 4 Black Body Responsivity vs. Chopping Frequency for a Typical n-Type Device Whose Initial Resistivity was .1 Ωcm. (Device 823N0.1)

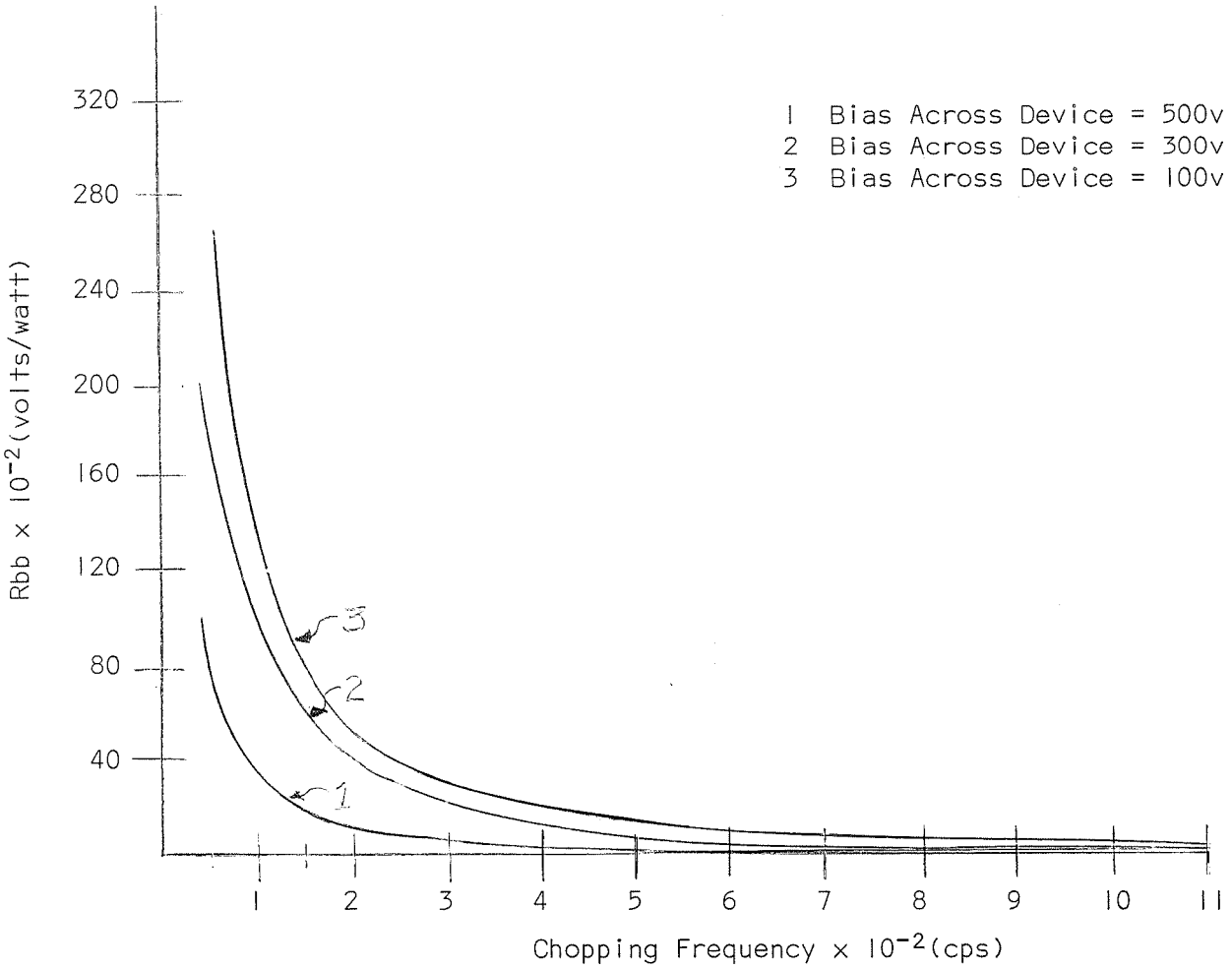


Figure 5 Black Body Responsivity vs. Chopping Frequency for a Typical p-Type Device Whose Initial Resistivity was 10 Ωcm. (Device 704P10)

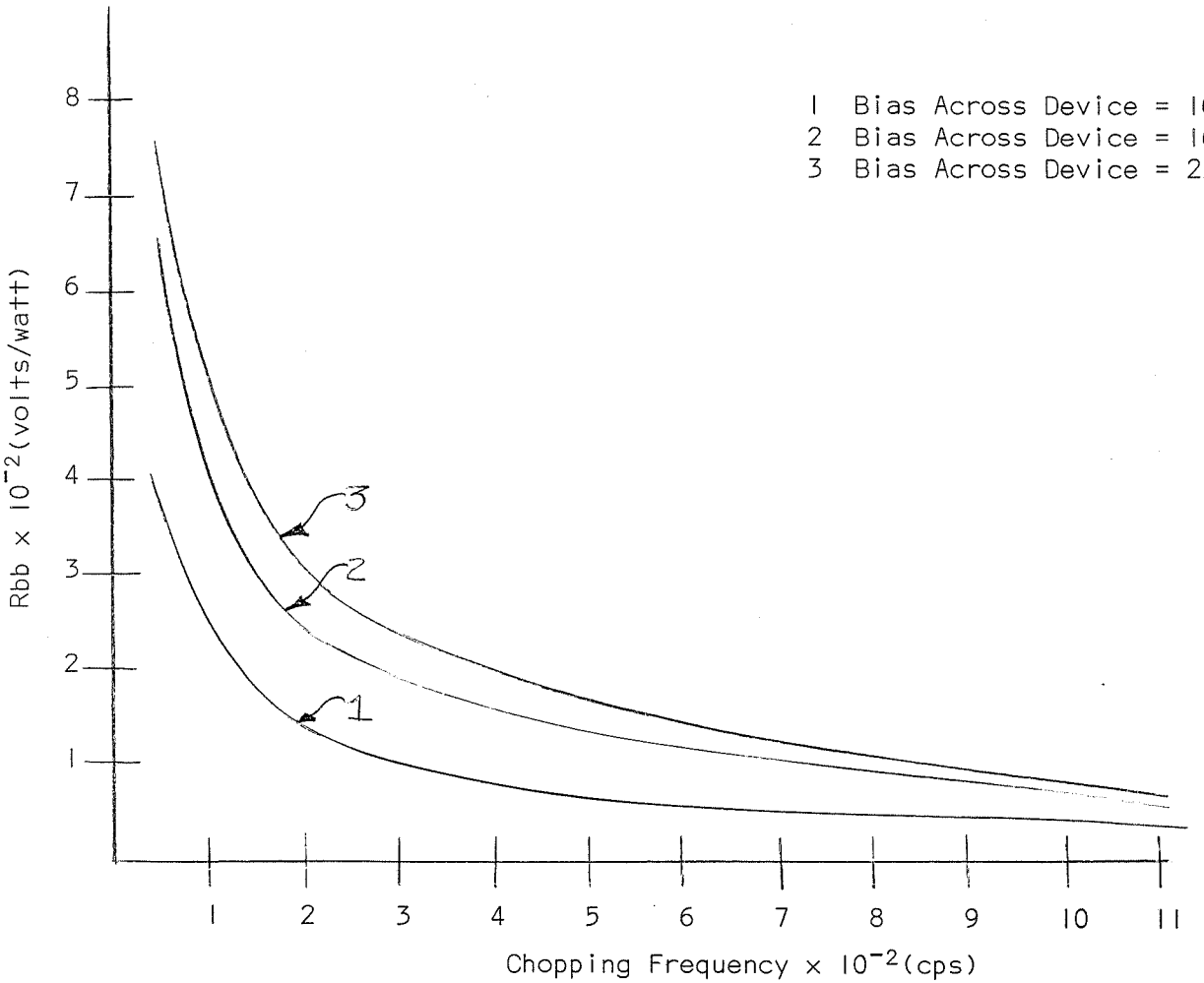


Figure 6 Black Body Responsivity vs. Chopping Frequency for a Typical p-Type Device Whose Initial Resistivity was 1 Ωcm. (Device 504P1.0)

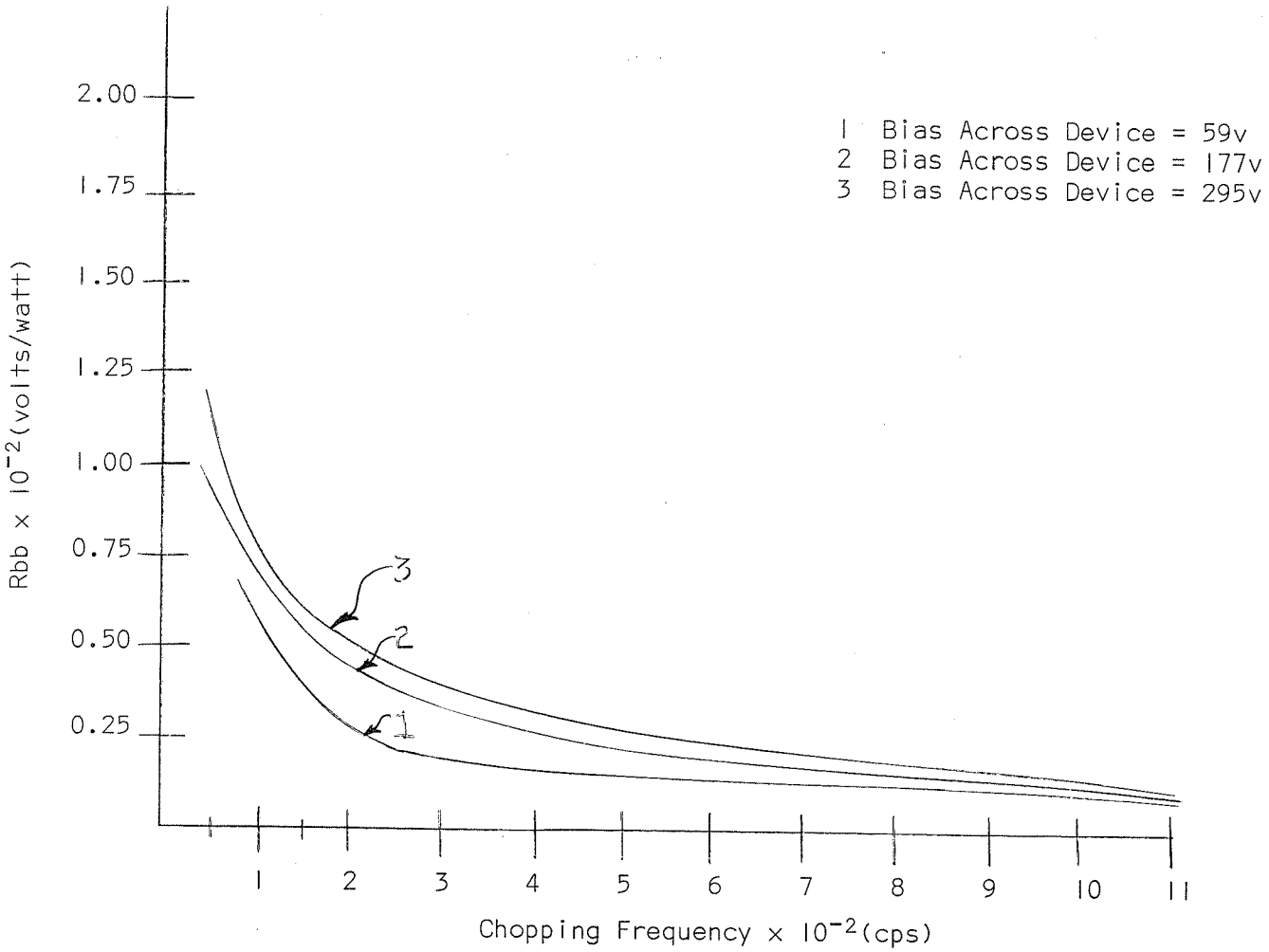


Figure 7 Black Body Responsivity vs. Chopping Frequency for a Typical p-Type Device Whose Initial Resistivity was .1 Ωcm. (Device 43IP0.1)

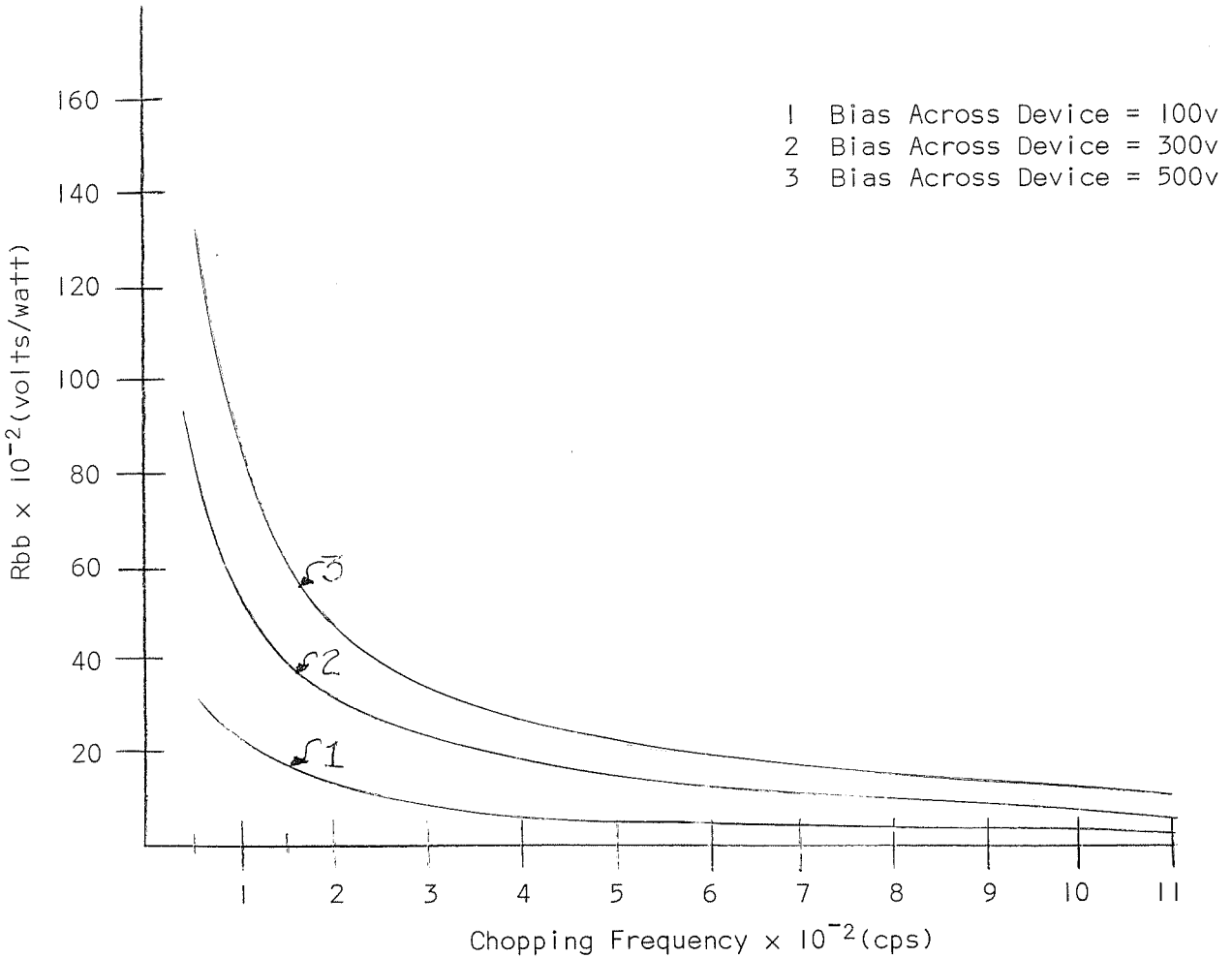


Figure 8 Black Body Responsivity vs. Chopping Frequency for a Typical n-Type Device Whose Initial Resistivity was .03 Ωcm. (Device 626N0.03)

77°K device resistance from the $10^{11}$ ohm range to the $10^{8}$ ohm range. Various duration annealings at 175°C and 275°C were used to remove radiation induced E($E_c$ - 0.42 eV) and A($E_c$ - 0.17 eV) centers respectively. The 100 Hz. black-body responsivity of devices fabricated from 1 ohm-cm n-type material ranged from 1 x $10^2$ to 100 x $10^2$ volts/watt. It was noted that the devices with highest black-body responsivity were those whose 77°K resistance was on the order of $10^8$ ohms. The black body responsivity trends for three different devices at 100 Hz. chopping frequency and 500 volt bias are summarized in Table I.

| Device Number | Rbb Before Annealing | Rbb After Annealing | Temperature and Duration of Annealing |
|---|---|---|---|
| 304N1.0 | 3.55 x $10^2$ | 9.1 x $10^2$ | 175°C - 25 hrs. |
| 303N1.0 | 0.88 x $10^2$ | 1.02 x $10^2$ | 175°C - 23 hrs. |
| | | 1.23 x $10^2$ | 175°C - 47 hrs |
| | | | 275°C - 10 min. |
| 301N1.0 | 9.8 x $10^2$ | 17.8 x $10^2$ | 175°C - 41.5 hrs. |
| | | | 275°C - 10 min. |

TABLE I

Two 1Ωcm n-type devices in particular, 332N1.0 and 333N1.0, were examined after successive annealing periods. Figures 9 and 10 show the effects of annealing these two devices at 175°C. As can be seen a definite peak in the black-body responsivity of each of these devices occurs after a total annealing time of from 18 to 24 hours. This peak is much more pronounced for lower radiation chopping frequencies. Thus the Rbb of these devices seems to increase for increased annealing time up to a certain limit beyond which it begins to decrease. Unfortunately device noise also increases in most cases with greater periods of annealing. We believe this to be a contact problem which we are actively working to eliminate.

Black-body responsivity was investigated as a function of bias voltage. The results are shown in Figures 11 and 12 and are seen to be linear in the regions of interest.

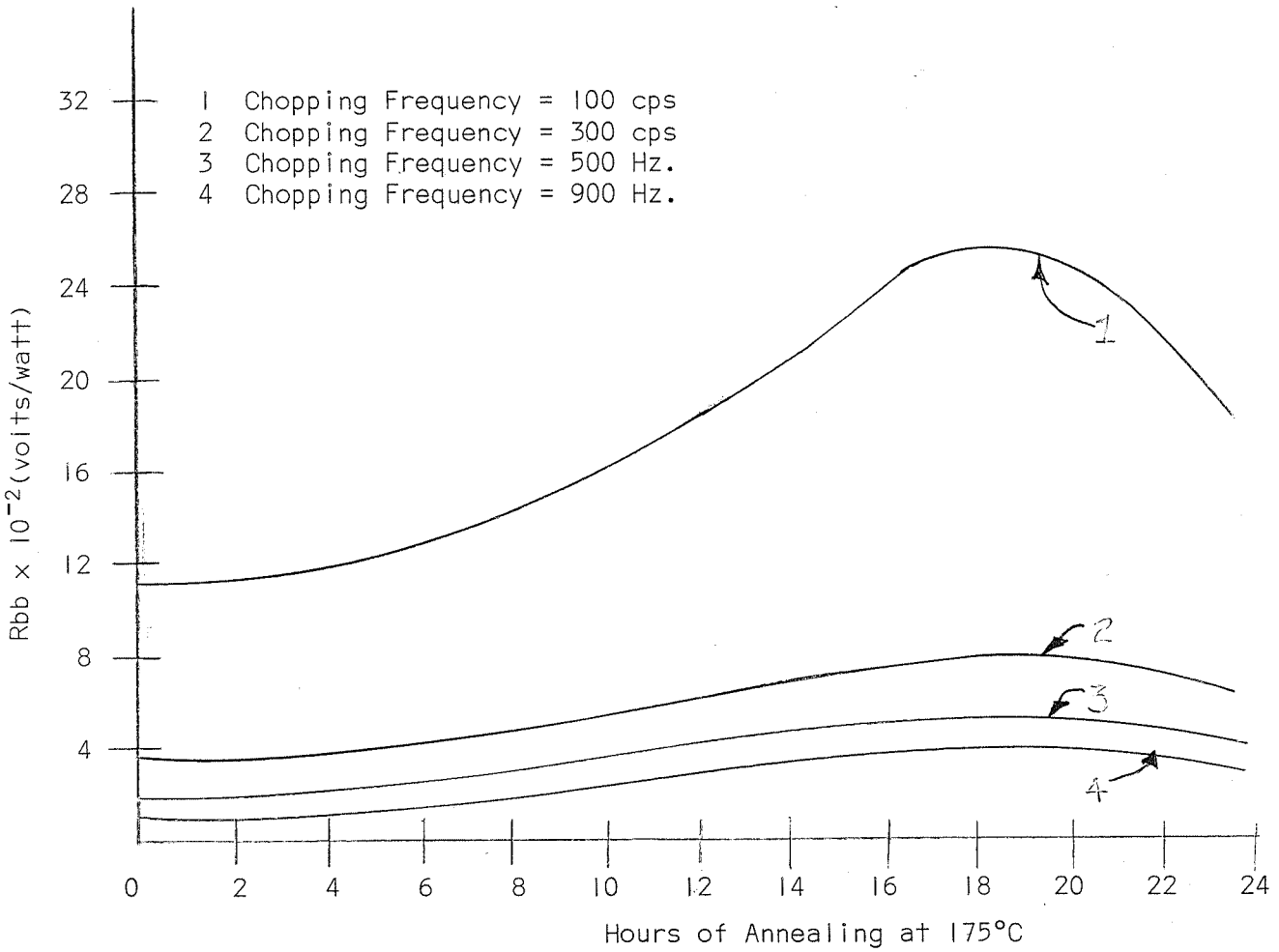


Figure 9 Black Body Responsivity vs. Hours of Annealing at 175°C (Device 332N1.0)

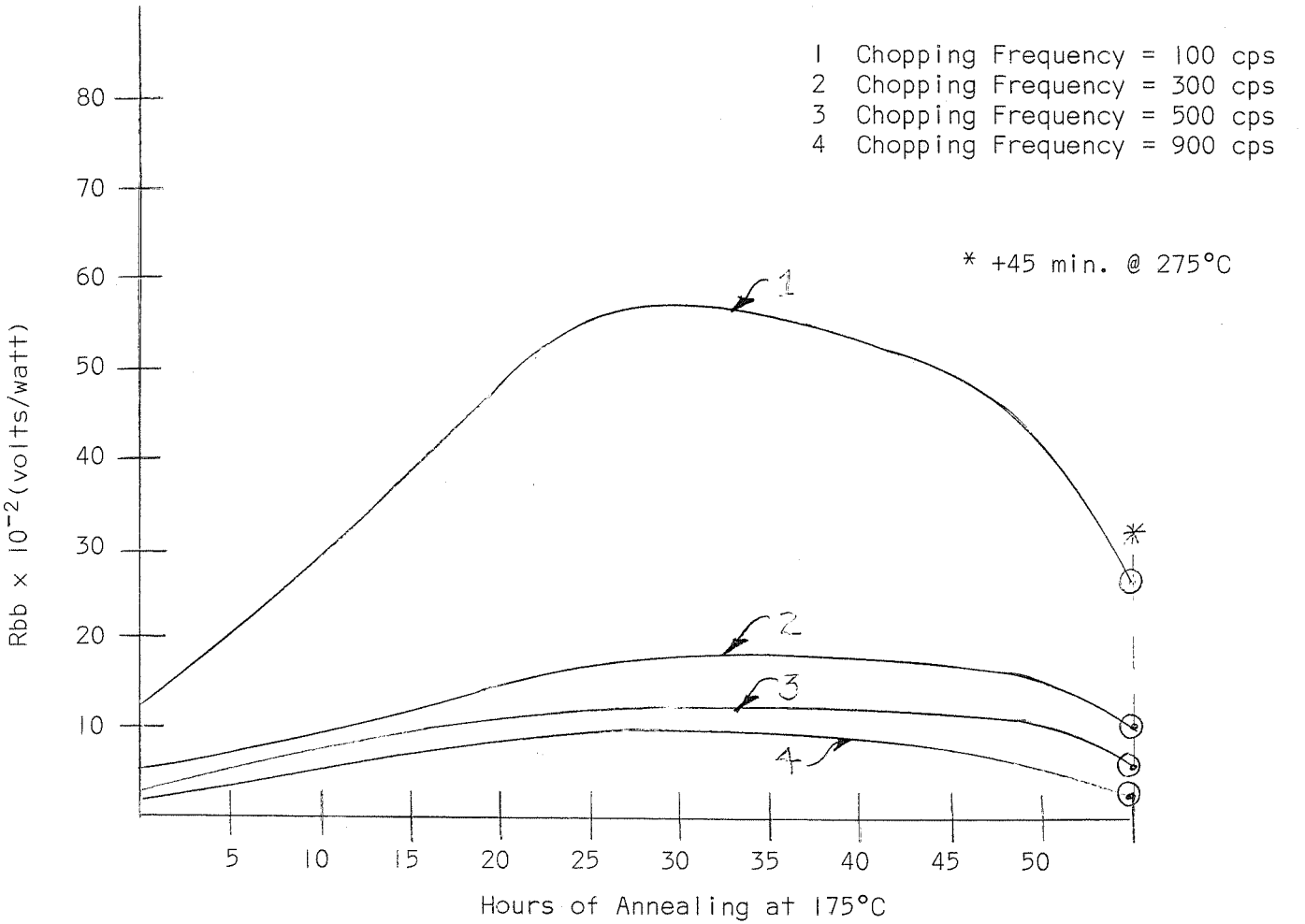


Figure 10 Black Body Responsivity vs. Hours of Annealing at 175°C (Device 333N1.0)

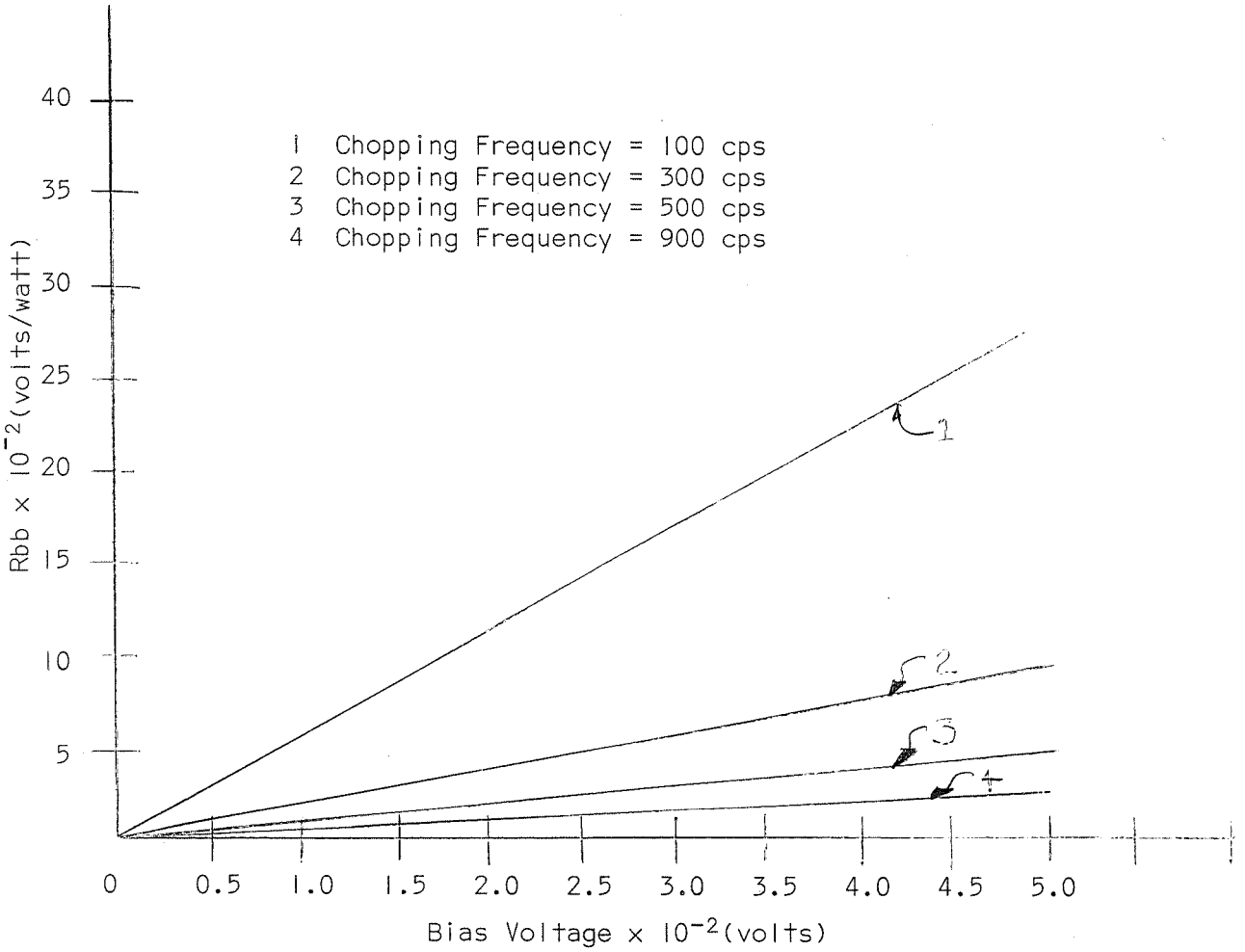


Figure 11 Black Body Responsivity vs. Bias Voltage (Device 332N1.0)

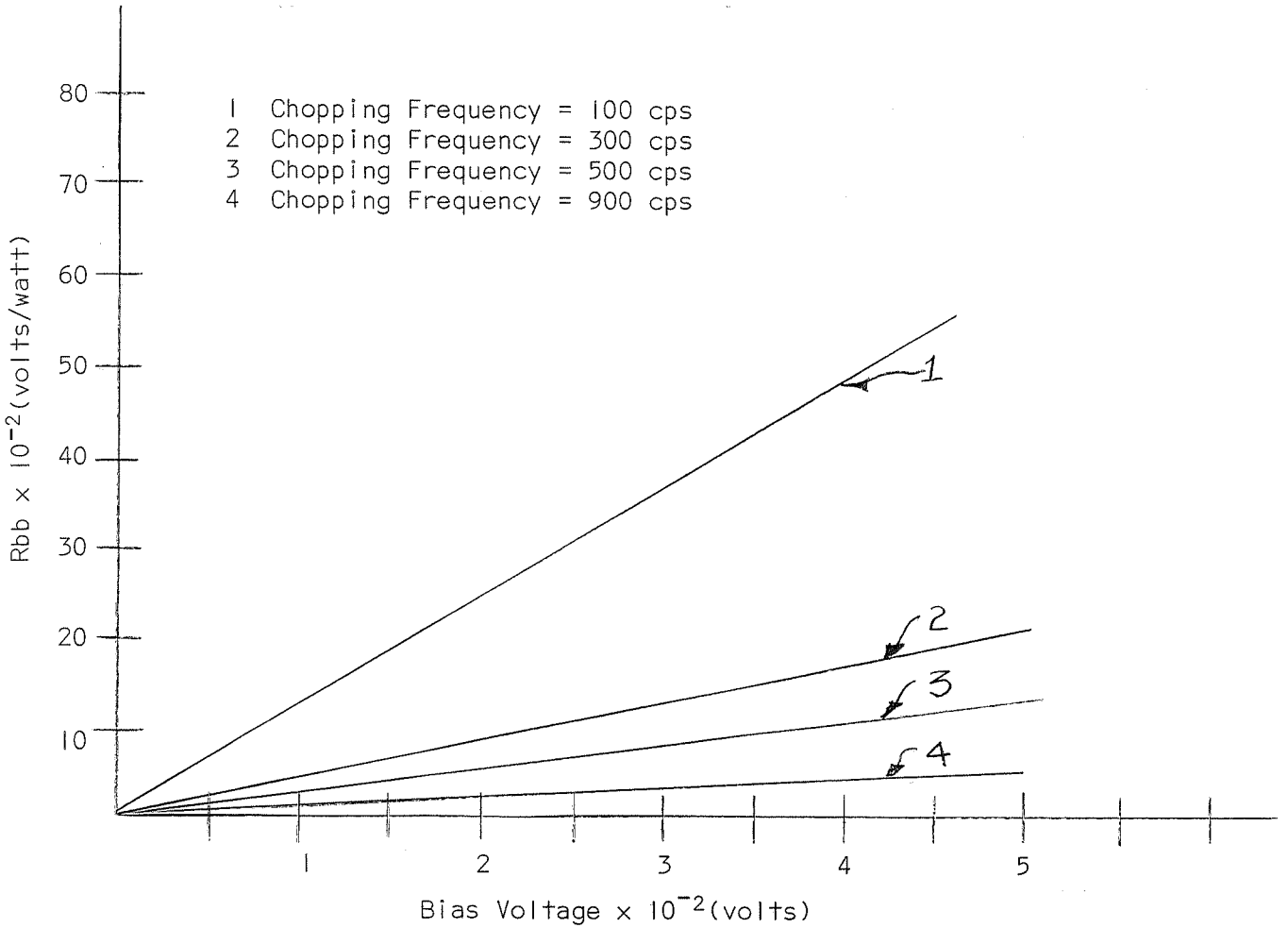


Figure 12 Black Body Responsivity vs. Bias Voltage (Device 333N1.0)

# SECTION V
# IMPROVED SYSTEM

Original plans called for the rebuilding of a Baird Atomic Infrared Spectraphotometer to be used as a monochrometer. A Jarrell-Ash model 82-410 monochrometer was recently procured and is now a part of a new and much more compact system. This system includes a new and much smaller black body source which was built in this lab. With both sources in the same system one need only rotate the dewar in which the device is situated so that either the monochromatic source or black body source is placed in front of the window on the dewar. This allows one to gather spectral or black body data simply by choosing the rotational position of the dewar.

A new liquid helium research dewar manufactured by Sulfrian Cryogenics Inc. replaces the original dewar and has three distinct advantages over the latter. They are:

(1) liquid helium temperature capability,

(2) a heated device holder allowing device operation at a temperature ranging from near 4°K to approximately 400°K,

(3) a spring loaded device holder and electrical contact. The last of these eliminates the need for mounting the devices on separate brass pads with conducting epoxy. Quite a great deal of trouble was encountered in using this epoxy since it became unusable and had to be changed after the device was annealed at an elevated temperature.

The monochrometer along with 4 different diffraction gratings provides a usable output the wavelength of which varies from 1.0 to 20 microns. The infrared source used for the monochrometer is an 1100°C silicon carbide Globar, and is enclosed in a water cooled jacket. A water-cooled plate with a small slit in it separates the source from the entrance slit of the monochrometer. This keeps the optical system from getting overheated. The output of the monochrometer is split into two separate infrared beams by means of a rotating silvered half disc which also serves as a 10 Hz. chopper. One beam is focused on a Model AT3 Baird Atomic bolometer by means of a front surface

spherical mirror. The second beam is focused on the device inside the dewar by means of a second front surface spherical mirror. The bolometer output is amplified by a 10 Hz. McDonald amplifier and is used as the reference for the relative spectral response determination. According to the manufacturer of the bolometer cell "Designed for radiation measurements in the 1 to 26 micron region, the Model AT-3 possesses flat spectral sensitivity characteristics over the entire range."

The entire system is mounted on a common base plate and is shown in diagramatic form in Fig. 13.

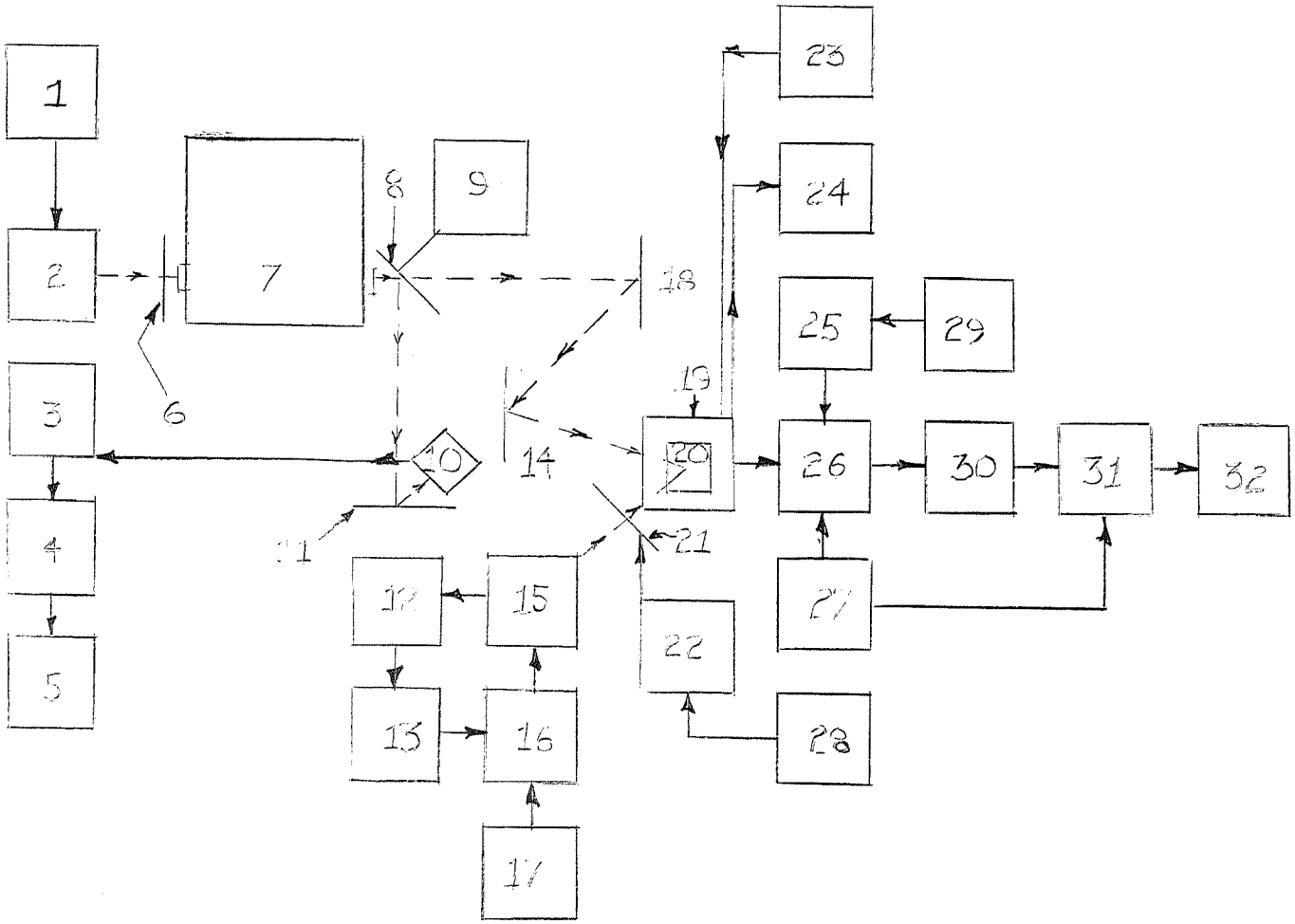


(See "Legend for Figure 13" for Identification)

Figure 13 Block Diagram of Consolidated Responsivity, Frequency Response, and Spectral Response Equipment

Legend for Figure 13

1. Globar Source Transformer
2. Globar Source
3. Bolometer 10 Hz. Amplifier
4. Bolometer Monitor Oscilloscope
5. Phase-Lock Microvoltmeter
6. Water-Cooled Shielding Plate
7. Monochrometer
8. 10 Hz. Chopper
9. 10 Hz. Chopper Motor
10. Bolometer
11. Concave Front Surface Mirror
12. Thermocouple
13. Temperature Controller
14. Front Surface Mirror
15. Black Body Source
16. Relay
17. Variac
18. Concave Front Surface Mirror
19. Dewar
20. Device
21. Black Body Source Chopper
22. Series Motor
23. Cold Finger Heater Power Supply
24. Cold Finger Thermocouple Millivoltmeter
25. Bias Supply Filter
26. Bias Circuit and Preamplifier
27. Signal Generator
28. Variac
29. Bias Supply
30. Device Monitor Oscilloscope
31. BNC Switch
32. Wave Analyzer, or Phase-Lock Microvoltmeter

## SECTION VI
## SPECTRAL RESPONSE

As was mentioned in Section II the spectral detectivity, $D^*_\lambda$, can be found from the relative spectral response, the black body responsivity, and the spectral and integrated black body power output. This system of calculation has the advantage of being independent of any spectral variation in the spectral output power of the monochromatic source used. The system that is in use in this laboratory compares the electrical output of a spectrally flat bolometer with that of the test device instantaneously; hence the calculation scheme is independent of time variations in the spectral output of the monochrometer also. The absolute accuracy of the system is dependent solely on the accuracy of the determination of the black-body responsivity. Figure 14 bears a plot of $D^*_\lambda$ as a function of wavelength for a test device. During the next semiannum we plan to test many devices of different type resistivities and resistances and ultimately compare them by comparing their $D^*_{\lambda,f}$ values. From this information we will determine the values of initial substrate resistivity and total high energy electron exposure which will optimize $D^*_{m,m}$.

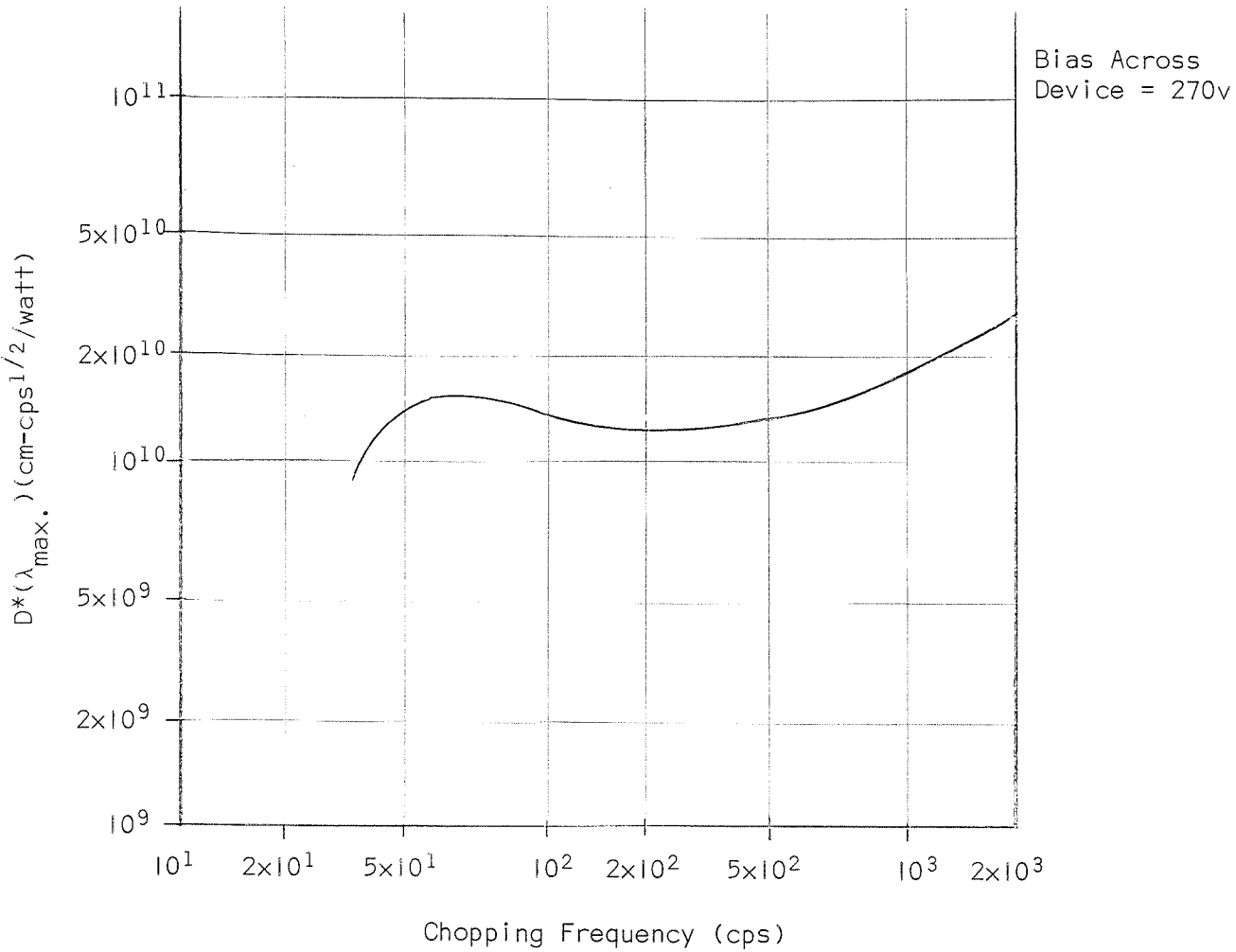


Figure 14 Spectral Detectivity at the Peak Wavelength ($D^*_{\lambda,m}$) vs. Chopping Frequency (Device 323NI.0)

## REFERENCES


1. P. W. Kruse, L. D. McGlauchlin, R. B. McQuistan, Elements of Infrared Technology, John Wiley & Sons, New York; 1962.

2. W. L. Eisenman, "Procedures Used in the Study of the Properties of Photodetectors," Naval Ordnance Laboratory Corona Report 541; July 1961.

3. R. B. McQuistan, "On an Approximation to Sinusoidal Modulation," Journal of the Optical Society of America, Vol. 48, No. 1; January 1958.

DISTRIBUTION LIST

| Copy No. | |
|---|---|
| 1-10 | National Aeronautics and Space Administration<br>Scientific and Technical Information Division<br>Code US, Attention: Winnie M. Morgan<br>Washington, D.C. 20546 |
| 11-12 | National Aeronautics and Space Administration<br>Langley Research Center<br>Langley Station<br>Hampton, Virginia 23365<br>Attention: Instrument Research Division |
| 13-14 | R. J. Mattauch |
| 15 | A. R. Kuhthau |
| 16 | C. M. Siegel |
| 17-21 | RLES Files |